FARADAY

Electrochemical *in situ* FT-IRRAS studies of a self-assembled monolayer of 2-(11-mercaptoundecyl)hydroquinone

Shen Ye, Akiko Yashiro, Yukari Sato† and Kohei Uosaki*
Physical Chemistry Laboratory, Division of Chemistry, Graduate School of Science, Hokkaido University, Sapporo 060, Japan

The potential-dependent structure change and irreversible anodic decomposition reaction of a 2-(11-mercaptoundecyl)hydroquinone ($H_2QC_{11}SH$) monolayer on a gold electrode surface in 0.1 mol l^{-1} $HClO_4$ solution has been investigated by electrochemical *in situ* FT-IRRAS. A number of bands with good signal-to-noise ratios have been observed at 1700–1100 cm^{-1} using p-polarization measurement but no bands were observed by s-polarization measurement when the potential was less than +1.2 V. The bands in this region corresponded well to the redox reaction of the terminal quinone group in the monolayer. The rate of this redox reaction was slow and its kinetics were discussed using the results obtained by the time-dependent FT-IRRAS measurements. When the electrode potential became more positive than +1.4 V, anodic current was present corresponding to oxidative decomposition of the monolayer, the IR bands at 1700–1100 cm^{-1} decreased in the p-polarization spectra and the bands at this frequency appeared in the s-polarization spectra. Bands at 2920 and 2850 cm^{-1} due to the C—H stretch and those at 1380 and 2342 cm^{-1} were also observed both by p- and s-polarization in this potential region. The bands at 1380 and 2342 cm^{-1} are attributed to the SO_2 stretch of alkylsulfonic acid, $R—SO_3H$, and CO_2, respectively. The results suggest that the monolayer was oxidized by anodic cleavage of an S—Au bond to form $R—SO_3H$ which possibly existed within the partially decomposed monolayer and was further oxidized to CO_2.

Quinone derivatives play very important roles in biological systems and their redox properties have been studied for a long time using electrochemical[1–8] and spectroscopic techniques.[9–12] Since electron transfer in biological systems usually involves molecules bound to a membrane, it is important to understand the electrochemical properties of quinone derivatives adsorbed on solid substrates with two-dimensional order.

The self-assembly method is now widely used to construct well ordered molecular layers.[13–15] The structures and properties of the self-assembled monolayers have been evaluated by many techniques, including electrochemical methods,[16–23] Fourier-transform IR reflection absorption spectroscopy (FT-IRRAS) under both *ex situ*[24–34] and *in situ*[35–38] conditions, *in situ* ellipsometry[39] and the electrochemical quartz crystal microbalance (EQCM) technique as well as the FT-IRRAS–EQCM combined technique.[40]

Hubbard and co-authors[41–47] studied the electrochemical behaviour and the structure of various quinone derivatives adsorbed on Pt(111) electrodes by several surface analysis techniques, including low energy electron diffraction (LEED), Auger electron spectroscopy and electron energy-loss spectroscopy (EELS). The self-assembled monolayers of quinone derivatives on gold electrodes have been also investigated by various groups.[48–55] The redox reaction of a quinone-terminated monolayer containing an alkyl chain is less reversible than that with no alkyl chain.[50,51] To understand the mechanism of the redox reaction of the self-assembled monolayers of quinone derivatives on an electrode and to clarify the role of the alkyl chain on the kinetics of the redox reaction, information on the potential dependence of the quinone monolayer structure is essential. One of the most useful techniques by which to obtain the structural information of adsorbed species on an electrode is *in situ* FT-IRRAS. FT-IRRAS measurements have been applied to study the structure of surface adsorbed species including ions such as cyanate,[56–58] bisulfate[59–61] and phosphate,[62–64] and neutral molecules such as CO.[65–67] Although it has been recognized that the *in situ* FT-IRRAS method is suitable to investigate the orientation and structure of the monolayer attached on the electrode in electrolyte solution, only a few reports of *in situ* FT-IRRAS studies of self-assembled monolayers are available.[35–39,54–56] One reason is the very strong IR absorption by water which inhibits the detailed study of the structure of the monolayer in the C—H stretching region.

In this study, we have constructed a self-assembled monolayer of a novel quinone-terminated molecule, 2-(11-mercaptoundecyl)hydroquinone (abbreviated as $H_2QC_{11}SH$, where H_2Q denotes the hydroquinone group), on a gold electrode and evaluated the redox property and oxidative decomposition process of the $H_2QC_{11}SH$ monolayer electrochemically as well as by *in situ* FT-IRRAS measurement.

Experimental

Synthesis of $H_2QC_{11}SH$

$H_2QC_{11}SH$ was synthesized following the procedure reported by Hickman *et al.*[50] 11-Bromo-1-(1,4-dimethoxybenzyl)undecanone was obtained by the reaction between 1,4-dimethoxybenzene (Wako Pure Chemicals) and 11-bromoundecanoyl chloride (Wako Pure Chemicals) in the presence of $AlCl_3$ (Merck) in dichloroethane (Wako Pure Chemicals). The resultant ketone was reduced by using palladium on carbon (Nakalai Tesque, Inc.). After demethylation, the terminal bromide group was converted to thiol (—SH) by using CH_3COSH (Wako Pure Chemicals). The crude thiol was purified by column chromatography by using silica gel. The final product ($H_2QC_{11}SH$) was characterized by ^1H NMR, IR and mass spectra. Analysis data for $H_2QC_{11}SH$ are: ^1H NMR ($CDCl_3$) δ 6.63 (m, 2 H), 6.56 (m, 1 H), 4.35 (s, 1 H), 4.32 (s, 1 H), 2.53 (m, 4 H), 1.60 (m, 2 H), 1.37–1.27 (m, 17 H); IR 3250, 3018, 2920, 2849, 2449, 1503, 1456, 1364, 1192 cm^{-1}; MS *m/z* 296 (M^+, base peak), 149, 136, 123.

† Present address: National Institute of Bioscience and Human Technology, 1-1 Higashi, Tsukuba, Ibaraki 305, Japan.

Electrochemical measurement

An Au(100) surface prepared by the Clavilier's method[68] was used as an electrode for electrochemical measurements. The diameter of the electrode was about 2 mm. Before each measurement, the electrode was annealed in gas–oxygen flame and quenched in N_2-saturated Milli-Q water. The surface condition was confirmed by a cyclic voltammogram in 0.1 mol l^{-1} $HClO_4$ and the real surface area was determined from the reduction peak of oxygen adsorption on the Au electrode. All the current densities are determined from the real surface area of the electrode. As the surface order is lost by the oxidation–reduction cycle, the electrode was annealed and quenched again, and the electrode was dipped into 1 mmol l^{-1} $H_2QC_{11}SH$ ethanol solution for 1 h to form the monolayer. After the adsorption process, the electrode was rinsed with ethanol and Milli-Q water and, finally, dried by blowing with N_2.

$HClO_4$ solution (0.1 mol l^{-1}) prepared from Suprapure reagent (Wako Pure Chemicals) and Milli-Q water were used as the electrolyte solution. An Ag/AgCl electrode or a quasi-reversible hydrogen electrode was used as the reference electrode. The potentials were measured with respect to the reversible hydrogen electrode (RHE). All the measurements were carried out at room temperature.

FT-IRRAS measurement

FT-IRRAS measurements were performed by using a BioRad FTS30 spectrometer equipped with an HgCdTe detector cooled with liquid nitrogen. A CaF_2 prism was used as an IR window and the incident angle was *ca.* 65° for p- and s-polarized IR radiation. To observe the spectroscopic behaviour in the low frequency region (<1100 cm^{-1}) where IR light is not transparent for a CaF_2 window, a ZnSe hemisphere window was used. A gold disk (diameter, 8 mm) was used as an electrode for FT-IRRAS measurements. Before FT-IRRAS measurement, the electrode was polished with alumina (0.05 mm) and rinsed with Milli-Q water. A spectroelectrochemical cell which allows the electrode to be pushed to the window with a micrometer without rotation of the electrode was employed for subtractively normalized interfacial Fourier-transform IR reflection-absorption spectroscopy (SNIFTIRS) measurement. The spectra were collected at the sample and reference potentials for 128 scans for eight or four times with a resolution of 4 cm^{-1}. Usually the collection of the spectra commenced 5 s after the potential was varied. In the experiment carried out to investigate the reaction kinetics, the time interval before collection of spectra was changed from 5 s to 10 min. The results are presented in the form of the normalized change of reflectance, $\Delta R/R$, which is equal to $(R_s - R_r)/R_s$ where R_s and R_r are the reflectance at the sample and the reference potential, respectively. The upward and downward peaks in the spectra mean that the species have disappeared or been generated, respectively, at the sample potential.

Results and Discussion

Structure change during the redox of the quinone group of the attached monolayer

Cyclic voltammogram. Fig. 1 shows a cyclic voltammogram of the $H_2QC_{11}SH$-modified Au(100) electrode in 0.1 mol l^{-1} $HClO_4$ solution. A pair of redox peaks, corresponding to the oxidation of hydroquinone to benzoquinone and the reduction of benzoquinone to hydroquinone, was observed. The peak separation (0.58 V) is much larger than those of mercaptohydroquinone (H_2QSH, <0.1 V),[48,49] 2,5-dihydroxybenzyl mercaptan (H_2QC_1SH, <0.1 V),[53,55] 2,5-dihydroxy-4-methylbenzyl mercaptan [$H_2Q(CH_3)C_1SH$, <0.1 V][55] and 2-(8-mercaptooctyl)hydroquinone (H_2QC_8SH, *ca.* 0.3 V).[50] It is clear that the long alkyl chain plays very important roles in the electrochemical redox reaction of the $H_2QC_{11}SH$-attached monolayer. Details of the effects of chain length, sweep rate and pH on the electrochemical characteristics of mercaptoalkylhydroquinone monolayers on gold electrodes will be reported elsewhere.[51]

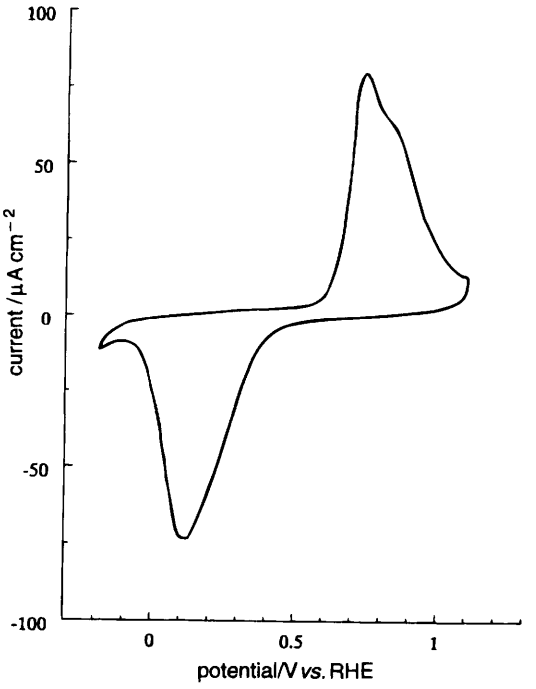

Fig. 1 Cyclic voltammogram of the $H_2QC_{11}SH$-modified Au(100) electrode in 0.1 mol l^{-1} $HClO_4$ solution. The scan rate was 0.1 V s^{-1}.

The amount of saturated adsorption calculated from the cyclic voltammogram was *ca.* 5.5×10^{-10} mol cm^{-2}, corresponding to one adsorbed $H_2QC_{11}SH$ molecule per 3.7 surface Au atoms. Hubbard *et al.* reported that the amounts of adsorption of $H_2Q(CH_3)C_1SH$ and H_2QSH on a Pt(111) electrode were 3.8×10^{-10} mol cm^{-2} and 2.6×10^{-10} mol cm^{-2}, respectively.[41] Their LEED study showed that the monolayer structure of the former was $2\sqrt{3} \times \sqrt{3}$ *R*30°. The amounts of adsorbed molecules on a gold electrode were reported for H_2QSH [$(2.7–4.3) \times 10^{-10}$ mol cm^{-2}],[48,49,53] H_2QC_1SH (3.0×10^{-10} mol cm^{-2}),[53] $H_2Q(CH_3)C_1SH$ (1.5×10^{-10} mol cm^{-2})[53] and H_2QC_8SH [$(3–5) \times 10^{-10}$ mol cm^{-2}].[50] The amount of adsorption of the $H_2QC_{11}SH$ monolayer is the largest, suggesting the self-assembled monolayer of $H_2QC_{11}SH$ on an Au electrode surface is very well packed. However, the crystallinities of the electrodes were different and, therefore, quantitative comparison must be done with care.

FT-IRRAS spectra. Fig. 2 shows *in situ* SNIFTIRS spectra obtained by using p- and s-polarized IR radiation. The sample potential was +1.0 V where the terminal group of adsorbed $H_2QC_{11}SH$ monolayer was expected to exist as the benzoquinone form and the reference potential was selected to be 0 V where the terminal group existed as hydroquinone. In the case of p-polarization (top curve in Fig. 2), a number of well defined bands were observed in the frequency region of 1700–1100 cm^{-1}. Two upward peaks at 1508 and 1456 cm^{-1} were found with similar intensity and another upward one was observed at 1206 cm^{-1}. For the downward bands, a very strong band at 1660 cm^{-1} and a small sharp band at 1600 cm^{-1} were observed and a broader one was found at 1303 cm^{-1}. On the other hand, no bands were observed in the case

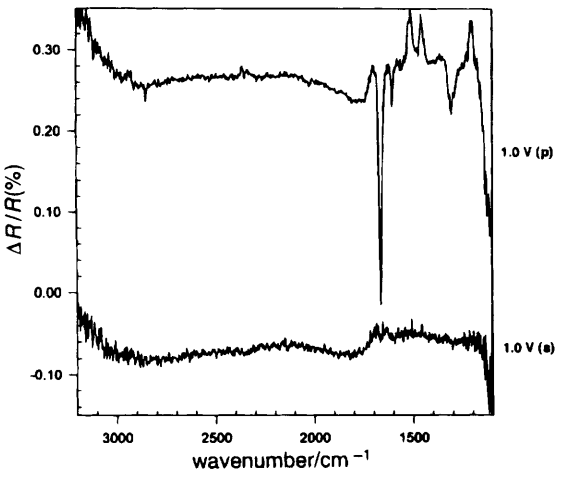

Fig. 2 *In situ* FT-IRRAS spectra of the $H_2QC_{11}SH$ monolayer adsorbed on a gold electrode obtained by p- (top curve) and s- (bottom curve) polarized light in 0.1 mol l^{-1} $HClO_4$ solution. The sample potential was +1.0 V and the reference potential was 0 V.

of s-polarization (bottom curve, Fig. 2). Thus, the bands observed with p-polarization in Fig. 2 should be of the attached monolayer. The bands appeared as a result of the IR absorption difference between the sample and reference potentials of the monolayer, *i.e.*, the difference between the benzoquinone and hydroquinone terminated monolayer.

Fig. 3 shows the SNIFTIRS spectra of the $H_2QC_{11}SH$-attached monolayer obtained at various potentials with p-polarization in the region of 3200–1100 cm^{-1}. No band was found in the potential region more negative than +0.6 V, where no oxidation of hydroquinone group took place. When the potential became more positive than +0.6 V, the IR bands appeared at 1700–1100 cm^{-1} as shown in Fig. 2. Clear bands were observed only in the 1700–1100 cm^{-1} frequency region

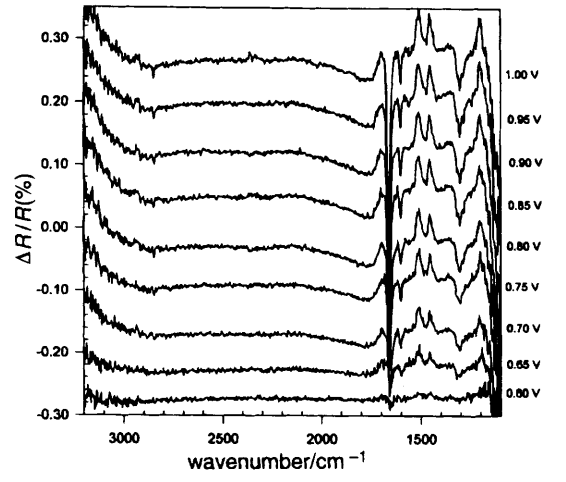

Fig. 3 *In situ* FT-IRRAS spectra of the $H_2QC_{11}SH$ monolayer adsorbed on a gold electrode at various sample potentials obtained by p-polarized light in 0.1 mol l^{-1} $HClO_4$ solution. The sample potentials are indicated near the respective spectra. The reference potential was 0 V.

when the potential was more negative than +1.2 V. The band intensity increased as the electrode potential became more positive and saturated around +1.0 V where the oxidation was complete. Thus, the potential dependence of the IR band intensity shows that these bands appeared as a result of the redox of the quinone moiety. The peak positions of these bands seemed to be independent of the electrode potential.

Assignment of the upward bands in the 1700–1100 cm^{-1} region. As described in the Experimental section, the upward and the downward bands in the SNIFTIRS spectra indicate the stronger IR absorption at the reference and sample potentials, *i.e.*, the IR absorption by hydroquinone and benzoquinone type monolayers, respectively. Thus, the three upward bands observed at 1508, 1456 and 1206 cm^{-1} should correspond to the IR absorption by the hydroquinone form in the $H_2QC_{11}SH$ monolayer.

Hubbard *et al.* performed an EELS study of the H_2QSH molecule adsorbed on a Pt(111) surface and found three bands at 1574, 1463 and 1171 cm^{-1} attributable to the hydroquinone form.[41] The band at 1171 cm^{-1} was assigned to the C—O stretch and those at 1463 and 1574 cm^{-1} were assigned to the C—C stretch of the benzene ring of the H_2QSH monolayer. The positions of these bands were similar to those in the present work. Sasaki *et al.* carried out an *in situ* SNIFTIRS study of an H_2QSH adsorbed at an Au electrode and observed many bands due to the hydroquinone form.[54] They assigned the IR absorption bands observed at 1207 and 1180 cm^{-1} to the C—O stretch and three bands observed 1445, 1497 and 1595 cm^{-1} to the C=C skeletal stretch of the benzene ring of the H_2QSH monolayer. Recently, however, the same group investigated the H_2QC_1SH monolayer adsorbed on an Au electrode by employing an ATR–FTIR system and found only three bands at 1501, 1455 and 1201 cm^{-1} for the hydroquinone form.[55] The quality of the spectra of the H_2QC_1SH monolayer was much better than that of the H_2QSH monolayer reported previously by Sasaki *et al.* The peak positions of the bands observed for the H_2QC_1SH monolayer are very similar to those of $H_2QC_{11}SH$ monolayer observed in this study. Thus, we can assign the two bands at 1508 and 1456 cm^{-1} to the benzene ring stretch of the $H_2QC_{11}SH$ monolayer, as those bands are typically observed for a 1,2,4-trisubstituted benzene ring[69–71] and the band at 1206 cm^{-1} to the C—O stretch of hydroquinone.[69–71] The extra bands reported by Sasaki *et al.* at 1180 and 1595 cm^{-1} may be due to the solution species as the stability of the H_2QSH monolayer is relatively low compared with the monolayers with alkyl chains. The assignments of these upward bands are summarized in Table 1.

Assignment of the downward bands in the 1700–1100 cm^{-1} region. Three downward bands observed at 1660, 1600 and 1303 cm^{-1} in the present IRRAS spectra (Fig. 2 and 3) are due to the oxidized form of the $H_2QC_{11}SH$ monolayer.

The very strong band at 1660 cm^{-1} can be assigned to the C=O stretch of quinone easily.[69–71] Bands at similar frequencies were reported for the benzoquinone (BQ) species in solution (1672 cm^{-1})[9–12] and the oxidized form of H_2QSH

Table 1 Assignment of IR absorption of upward bands

assignment		wavenumber/cm^{-1}	method	ref.
benzene ring stretch	H_2QSH on Pt(111)	1463, 1574	EELS	41
	H_2QSH on Au	1445, 1497, 1595	*in situ* IRRAS	54
	$H_2QC_{11}SH$ on Au	1455, 1501	*in situ* ATR-FTIR	55
	$H_2QC_{11}SH$ on Au	1456, 1508	*in situ* IRRAS	this study
C—O stretch	H_2QSH on Pt(111)	1171	EELS	41
	H_2QSH on Au	1207, 1180	*in situ* IRRAS	54
	$H_2QC_{11}SH$ on Au	1200	*in situ* ATR-FTIR	55
	$H_2QC_{11}SH$ on Au	1206	*in situ* IRRAS	this study

(1647 cm^{-1})[54] and H_2QC_1SH (1650 cm^{-1})[55] monolayers. The sharp band at 1600 cm^{-1} should be assigned to the C=C stretch of the quinone ring.[69–71] An IR absorption band around 1600 cm^{-1} was also observed by Davies *et al.*[9] and Bauscher *et al.*[12] for BQ in solution and was assigned to the C=C stretch. Although the ATR–FTIR spectra of the H_2QC_1SH monolayer reported by Bae *et al.* resembled the present result of the $H_2QC_{11}SH$ monolayer, no band corresponding to that at 1600 cm^{-1} was found.[55] This result may reflect the orientation difference between the two monolayers. Sasaki *et al.* found the bands, which they assigned to the C=C stretch of the quinone ring of the oxidized form of the H_2QSH monolayer, not around 1600 cm^{-1}, but at lower frequency (1531 and 1561 cm^{-1}).[54] The reason for this discrepancy is not clear. The small broader band at 1303 cm^{-1} can be assigned to the C—C stretch of the quinone ring of the oxidized form of the $H_2QC_{11}SH$ monolayer,[27–29] as a band assigned to the C—C stretch of the quinone ring was reported for BQ species in solution (1302 cm^{-1}),[9] the H_2QSH (1306, 1286 cm^{-1}) monolayer and the H_2QC_1SH (1293 cm^{-1}) monolayer.[19,20] The assignments for the downward bands are summarized in Table 2.

Potential dependence of peak intensities and kinetics of the redox process of the $H_2QC_{11}SH$ monolayer. The mechanism of the redox reaction of molecules with a quinone group both in solution and of the adsorbed state is very complicated as reported previously.[1–8,12] At least two elementary steps, electron transfer and protonation, are included in the redox process of a quinone moiety. Thus, the rate of the redox reaction of quinone strongly depends both on the electrode potential and solution pH. A large peak separation (0.58 V) observed in the cyclic voltammogram of the gold electrode modified with the $H_2QC_{11}SH$ monolayer in acidic solution shows that the redox reaction of the quinone moiety is rather slow (Fig. 1). The peak separation of the $H_2QC_{11}SH$ monolayer-modified gold electrode in alkaline solution was nearly zero, suggesting that the protonation step of the terminal quinone group in the $H_2QC_{11}SH$ monolayer is the rate-controlling step in acidic solution. This is in contrast to the result observed at the gold electrode modified with the H_2QSH monolayer where the peak separation is small in solutions of high pH. This difference should be related to the existence of the long alkyl chain in the $H_2QC_{11}SH$ monolayer.

Fig. 4 shows the potential dependence of the degree of oxidation of the quinone moiety of the $H_2QC_{11}SH$ monolayer determined electrochemically and by *in situ* FT-IRRAS. The solid line represents the normalized anodic charge, *i.e.* the charge passed up to a given potential divided by the total charge passed up to +1.1 V, in the positive going sweep of the cyclic voltammogram shown in Fig. 1. The black circles show the normalized intensity of the IR band at 1660 cm^{-1} due to the C=O stretch of the quinone, *i.e.*, the band intensity at a given potential divided by that at +1.2 V obtained from Fig.

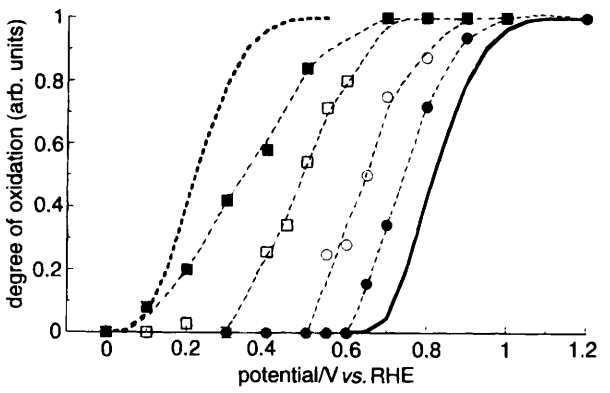

Fig. 4 The potential dependence of the degree of oxidation of the quinone moiety of the $H_2QC_{11}SH$ monolayer on a gold electrode in 0.1 mol l^{-1} $HClO_4$ solution determined electrochemically and by *in situ* FT-IRRAS. Solid line, the normalized anodic charge which is the charge passed up to a given potential divided by the total charge passed up to +1.1 V in the positive going sweep of the cyclic voltammogram shown in Fig. 1. The black circles and white circles are the normalized intensities of the IR band at 1660 cm^{-1} due to the C=O stretch of the quinone, which is the band intensity at a given potential divided by that at +1.2 V obtained with 5 s and 5 min, respectively, waiting time before the collection of the spectra after the potential was varied from 0 V to a given potential. Dotted line, the degree of oxidation determined as (1 − the normalized cathodic charge) where the normalized cathodic charge is the charge passed up to a given potential divided by the total charge passed up to −0.1 V in the negative going sweep of the cyclic voltammogram shown in Fig. 1. The black squares and white squares are the normalized intensities of the IR band at 1660 cm^{-1} due to the C=O stretch of the quinone obtained with 5 s and 5 min, respectively, waiting time before the collection of the spectra after the potential was varied from +1.2 V to a given potential.

3. Although both values should reflect the degree of oxidation of the quinone moiety, they do not correspond with each other. The oxidation seems to be complete at less positive potential in the *in situ* FT-IRRAS measurement. Since the cyclic voltammogram was obtained with a sweep rate of 0.1 V s^{-1} and there was a 5 s waiting time before the collection of the spectra after the potential was varied in the *in situ* FT-IRRAS measurement, the discrepancy between the degree of oxidation determined electrochemically and that determined by *in situ* FT-IRRAS may be due to the slow kinetics of the anodic oxidation of the quinone. To see the effect of the slow kinetics, IR spectra were obtained with a 5 min waiting time before the collection of the spectra after the potential was varied. The results are shown in Fig. 4 as the normalized intensity of the IR band at 1660 cm^{-1}, represented by open circles. The degree of oxidation at a given potential increased with increasing waiting time, confirming that the discrepancy was due to the slow kinetics. The difference of the potential of 50% oxidation between the electrochemically determined value (+0.81 V) and that obtained by the *in situ* FT-IRRAS measurement with a 5 min waiting time (+0.64 V) is *ca.* 0.17 V. This effect seemed to be more pronounced in the reduction

Table 2 Assignment of IR absorption of downward bands

assignment		wavenumber/cm^{-1}	method	ref.
C=O stretch	BQ in solution	1672	IR transmission	9–12
	H_2QSH on Au	1647	*in situ* IRRAS	54
	H_2QC_1SH on Au	1650	*in situ* ATR-FTIR	55
	$H_2QC_{11}SH$ on Au	1660	*in situ* IRRAS	this study
quinone C=C stretch	BQ in solution	1592	IR transmission	9, 12
	H_2QSH on Au	1531, 1561	*in situ* IRRAS	54
	$H_2QC_{11}SH$ on Au	1600	*in situ* IRRAS	this study
C—C stretch	BQ in solution	1302	IR transmission	9
	H_2QSH on Au	1286, 1306	*in situ* IRRAS	54
	H_2QC_1SH on Au	1293	*in situ* ATR-FTIR	55
	$H_2QC_{11}SH$ on Au	1303	*in situ* IRRAS	this study

process. The dotted line in Fig. 4 shows the degree of oxidation determined as (1 − the normalized cathodic charge) where the normalized cathodic charge means the charge passed up to a given potential divided by the total charge passed up to −0.1 V in the negative-going sweep of the cyclic voltammogram shown in Fig. 1. The *in situ* FT-IRRAS measurements were carried out with the reference potential of +1.2 V where the terminal group existed as the oxidized, *i.e.* quinone, form with two different waiting times, 5 s and 5 min. The normalized intensities of the IR band at 1660 cm^{-1}, *i.e.* the band intensities at given potentials divided by that at 0 V, are also shown in Fig. 4, for a waiting time of 5 s (black square) and of 5 min (white square). The longer the waiting time, the smaller the degree of oxidation, showing that the reduction of quinone to hydroquinone was completed at less negative potentials. In this case, the difference of the potential of 50% reduction between the electrochemically determined value (+0.21 V) and that obtained by the *in situ* FT-IRRAS measurement with a 5 min waiting time (+0.48 V) is *ca.* 0.27 V, which is larger than that of the oxidation process by 0.1 V, showing the reduction process to be slower than the oxidation process.

It may be thought, however, that the waiting time dependent FT-IRRAS behaviour is simply due to the long time constant of the IR cell because of the thin electrolyte layer. This is not the case as no waiting time dependent FT-IRRAS behaviour was observed for a waiting time of 5 s to 10 min at the 11-ferrocenylundecane-1-thiol ($FcC_{11}SH$) monolayer on gold which gives a symmetric redox peak in the cyclic voltammogram.[40,75] Thus, the results shown in Fig. 4 should really reflect the slow kinetics of the redox reaction, reduction in particular, of the $H_2QC_{11}SH$ monolayer. In fact, it was found that the peak separation in the CV became smaller as the scan rate was reduced and the shift of the reduction peak was larger than that of the oxidation peak.[51]

This was further confirmed by the time-dependent FT-IRRAS measurements. Fig. 5 shows the intensity of the IR band at 1660 cm^{-1} which corresponds to the C=O stretch of quinone obtained after the potential was pulsed from the reference potential of +1.2 to +0.5 V (white circle) and +0.1 V (black circle). The peak was upward because the quinone form at +1.2 V was converted to the hydroquinone form at +0.5 and +0.1 V. Thus, although the vertical axis of Fig. 5 shows the intensity of the C=O stretch band, it actually represents the amount of hydroquinone form. It took more than 5 min to reach a steady value when +0.5 V was applied but the band intensity reached a steady value quickly when +0.1 V was applied. These results clearly show that the waiting time dependence of the spectra is due to the slow kinetics. If the time delay was due to the cell configuration, one would expect a longer time constant for the larger overpotential.

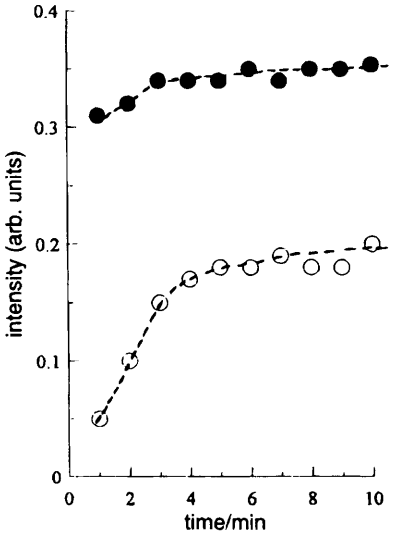

Fig. 5 The time dependence of the IR band intensity of C=O stretch at 1660 cm^{-1} of the $H_2QC_{11}SH$ monolayer adsorbed on a gold electrode after the potential was pulsed from reference potential of +1.2 to +0.5 V (white circle) and +0.1 V (black circle)

FT-IRRAS behaviour in the other frequency region. Note that no clear bands were observed in the frequency region between 3200 and 2800 cm^{-1}, where the bands due to the C—H stretching vibration should be observed, when the anodic potential was more negative than +1.2 V (Fig. 3). This result is quite different from those observed at the ferrocene-terminated alkyl thiolate monolayers with the same alkyl chain length, *i.e.* 11-mercaptoundecyl ferrocenecarboxylate ($FcCOOC_{11}SH$)[36] and 11-ferrocenenylundecane-1-thiol ($FcC_{11}SH$),[40,75] on a gold electrode. In the case of ferrocene-terminated monolayers, the IR absorption of C–H stretch of the methylene group decreased as the terminal ferrocene group was oxidized to the ferricinium cation, showing the orientation of the alkyl chain changed as the oxidation state of the ferrocene group changed. One possible reason for the different vibration features in the C–H stretch region for the two monolayers with different terminal groups (ferrocene and hydroquinone) should be the charge of the terminal groups. The interaction between the terminal group and the electrode and, therefore, the orientation of the alkyl chain should be strongly affected by the charge of the terminal group. The terminal group of the ferrocene-terminated monolayer is neutral in the reduced form but has positive charge in the oxidized form, while both the reduced and oxidized forms are neutral in the case of the hydroquinone-terminated monolayer. The other possible reason is the difference in the size of ions associated with the redox of terminal groups. While the relatively large anion moves in and out during the oxidation and the reduction, respectively, of the ferrocene moiety, the proton is associated with the redox of quinone/hydroquinone.

A ZnSe hemisphere window was used to observe the IR reflection absorption features in the lower frequency region instead of the CaF_2 window because the latter is not transparent for light of frequency lower than 1100 cm^{-1}. A broad downward band was observed around 1100 cm^{-1} (Fig. 6). This band is considered to be due to the perchlorate ion in solution.[76] The downward peak corresponds to an increase of perchlorate ion concentration near the electrode in the positive potential region. As the electrode potential becomes more positive, the positive charge of the electrode increases and perchlorate ion is attached to the electrode surface.

Oxidative decomposition of the $H_2QC_{11}SH$ monolayer on gold

Cyclic voltammogram. The monolayer was irreversibly oxidized when the anodic potential limit of the cyclic voltammogram was extended to more positive potential. As shown in Fig. 7, anodic current began to flow at *ca.* +1.4 V and the current increased rapidly as the potential became more positive. A peak due to the reduction of surface oxide was observed at +1.15 V in the reverse scan if the anodic scan limit was extended to +1.6 V (dotted line). A peak at +0.18 V which corresponds to the reduction of the quinone moiety in the monolayer started to decrease and a new reduction peak appeared at +0.65 V. When the anodic scan limit became as positive as +1.8 V, the peak at +0.18 V disappeared and the reduction peak at +0.65 V became more marked (broken line). The oxidation peak of the hydroquinone form of the $H_2QC_{11}SH$ monolayer at +0.76 V became somewhat broader and shifted only slightly to a more negative potential. As a result, the peak separation decreased from the initial value of 0.58 V to *ca.* 0.15 V (Fig. 7).

These results show that the monolayer was partially decomposed by the anodic oxidation. There are at least two

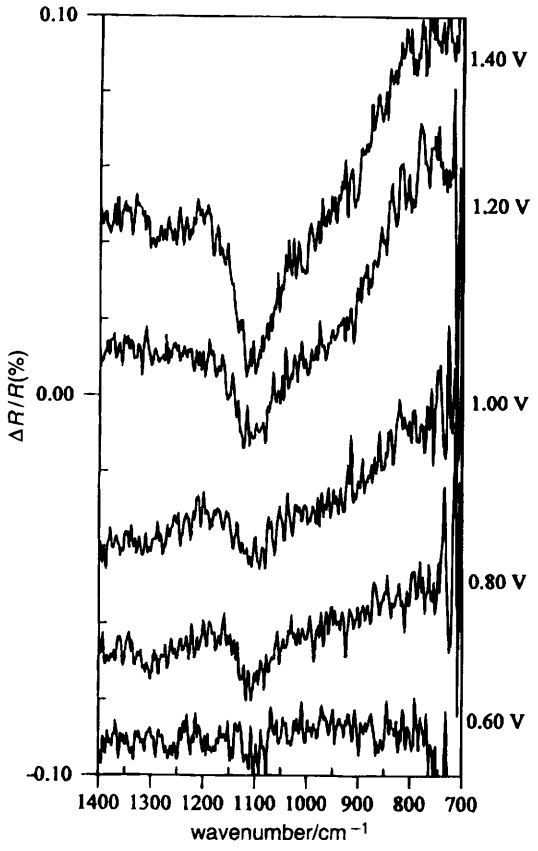

Fig. 6 *In situ* FT-IRRAS spectra of the gold electrode modified with the $H_2QC_{11}SH$ monolayer at various sample potentials obtained by using a ZnSe window with p-polarized light in 0.1 mol l^{-1} $HClO_4$ solution. The sample potentials are indicated near the respective spectra. The reference potential was 0 V.

possibilities for the new reduction peak at +0.65 V. One possibility is that the peak is due to the reduction of the quinone group of the partially decomposed $H_2QC_{11}SH$ monolayer. The reduction peak of the $H_2QC_{11}SH$ monolayer with lower coverage appeared at a similar position.[51] As the monolayer coverage decreased, free space among the alkyl chains increased and the hydrophobic nature of the monolayer decreased. Thus, the proton in solution should become more accessible to the quinone moiety and the reduction reaction proceeds more easily, resulting in the shift of the reduction peak to a more positive potential. There is also a possibility that the peak is due to the reduction of the decomposed fragments containing the quinone moiety in solution. Actually, the new peak position is very close to the value

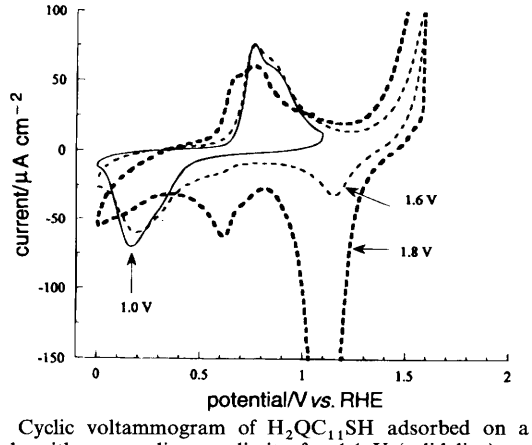

Fig. 7 Cyclic voltammogram of $H_2QC_{11}SH$ adsorbed on a gold electrode with an anodic scan limit of +1.1 V (solid line), +1.6 V (dotted line) and +1.8 V (broken line).

reported for the reduction of BQ in aqueous solution (pH 1).[77–79]

FT-IRRAS spectra of the decomposition process of the $H_2QC_{11}SH$ monolayer. *In situ* FT-IRRAS measurement was carried out to obtain more detailed information on the decomposition reaction process of the $H_2QC_{11}SH$ monolayer.

Fig. 8 (p-polarization) and Fig. 9 (s-polarization) show the *in situ* FT-IRRAS spectra obtained at relatively positive sample potentials. When the potential was more negative than +1.4 V, the spectra obtained by p- and s-polarization were the same as those obtained at +1.0 V (Fig. 2). When the potential was made more positive than +1.4 V, where the anodic current due to the oxidative decomposition of the monolayer flowed (Fig. 7), the IRRAS spectra of both by p- and s-polarization measurements changed greatly. Two new upward bands at 2850 and 2920 cm^{-1} were observed both by p- and s-polarization when the potential became more positive than +1.4 V and the intensities of these bands increased as the potential became more positive. The IR bands in the frequency region of 1700–1100 cm^{-1} observed by

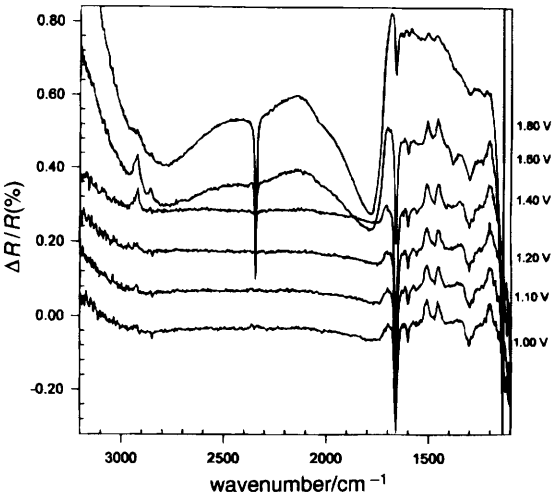

Fig. 8 *In situ* FT-IRRAS spectra of the $H_2QC_{11}SH$ monolayer adsorbed on a gold electrode in 0.1 mol l^{-1} $HClO_4$ solution at relatively positive sample potentials obtained by p-polarized light. The sample potential of each spectrum is indicated near the spectrum. The reference potential was 0 V.

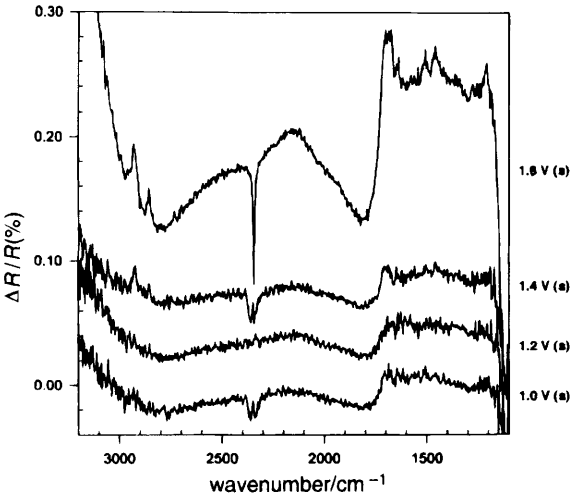

Fig. 9 *In situ* FT-IRRAS spectra of the $H_2QC_{11}SH$ monolayer adsorbed on a gold electrode in 0.1 mol l^{-1} $HClO_4$ solution at relatively positive sample potentials obtained by s-polarized light. The sample potential of each spectrum is indicated near the spectrum. The reference potential was 0 V.

p-polarization (Fig. 3) started to decrease at +1.4 V and became much weaker at +1.8 V. At the same time, a number of bands appeared in the s-polarization spectra in this frequency region. Their peak positions were similar to those observed in the p-polarization spectra shown in Fig. 3, although their intensities were weaker. Furthermore, a new sharp downward band at 1383 cm^{-1} and a very strong band at 2342 cm^{-1} were observed by p-polarization when the potential was more positive than +1.4 V. The band at 2342 cm^{-1} was observed also by s-polarization measurement.

The bands at 2850 and 2920 cm^{-1} observed by both p- and s-polarization should be attributed to the C—H symmetric and asymmetric, respectively, stretching vibrations of methylene group.[69,70] As already described, these bands were not observed in the spectra obtained both by p- and s-polarization measurements in the less positive potential region where only the redox of the quinone group of the $H_2QC_{11}SH$ monolayer took place, as shown in Fig. 2 and 3. Since the s-polarized IR radiation is inactive for the species adsorbed on the surface and the p-polarized radiation is active both for surface species and solution species,[80] these two bands should be due to the species in solution, *i.e.* decomposed fragments of the $H_2QC_{11}SH$ monolayer.

As described in the preceding sections, the bands observed in the 1700–1100 cm^{-1} frequency region corresponded well to IR absorption by the terminal quinone moiety of the $H_2QC_{11}SH$ monolayer. Since the main features in the vibration spectra in this frequency region were observed both by p- and s-polarization measurements at a very positive potential (Fig. 8 and 9), there existed some species in solution with a quinone group near the electrode after oxidative decomposition of the monolayer.

The band at 1383 cm^{-1} was observed only when the potential was more positive than +1.4 V, where the monolayer was oxidized. A band at nearly the same frequency was also observed when the monolayers of $FcC_{11}SH$ and dodecanethiol ($CH_3C_{11}SH$) on a gold electrode were anodically decomposed,[40,75] suggesting this band is related to the decomposition products of self-assembled monolayers of thiol derivatives. Porter and co-workers investigated the electrochemical desorption of *n*-alkanethiol monolayers from a polycrystalline gold electrode in anodic and cathodic potential regions by electrochemical measurements.[81,82] They proposed a mechanism by which the *n*-alkanethiol adsorbed at a gold electrode was oxidized into alkylsulfinic acid, RSO_2H, in an acidic solution at a positive potential region by comparing the charges for oxidative and reductive desorption processes. Huang *et al.* found alkylsulfonate by using FT-mass spectrometry after the gold surface, modified by the *n*-alkylthiolate self-assembled monolayer, was irradiated by a UV laser.[83–85] Recently, we confirmed the cleavage of the Au—S bond of the mercaptoalkanenitrile monolayer in its oxidative decomposition by XPS measurement.[56] The asymmetric and symmetric stretch vibrations of the SO_2 group are observed in the frequency regions of 1400–1300 cm^{-1} and 1200–1100 cm^{-1},[69–70] respectively, and the bands appear in the higher frequency region if a substituent with a higher electronegativity is bonded.[86–93] The bands of SO_2 vibration absorption of anhydrous sulfonic acid, R–SO_2–OH, were found at 1350–1375 cm^{-1} (asymmetric stretch) and 1165–1185 cm^{-1} (symmetric stretch).[69,70,94] The S=O stretch of the sulfinic acids was reported to appear at 1090–990 cm^{-1}.[69,70,94] Thus, the band at 1383 cm^{-1} observed in the present study can be attributed to the SO_2 asymmetric stretch of alkylsulfonic acid, R–SO_2–OH, which was formed as a product of oxidative cleavage of the Au—S bond. It is known that the IR band of sulfonic acid shifts to lower frequency region when it is hydrated and the asymmetric stretching band should be observed at *ca.* 1230–1120 cm^{-1}.[69,85,86] The peak position found in the present result shows that the R–SO_3H species were not hydrated, suggesting that they should exist in the partially decomposed monolayer near the electrode surface where the hydration is hindered because of the quasi-hydrophobic environment. The absence of the band due to the symmetric stretch of SO_2 in the present study is reasonable as the CaF_2 window has low transparency for the IR light in the frequency region near 1200 cm^{-1}. Furthermore, the production of alkylsulfinic acid, RSO_2H, proposed by Widrig *et al.*[81] was neither confirmed nor denied because the band should appear in a frequency region too low for the present measurements. Weisshaar *et al.* studied oxidative decomposition of the mercaptoethanol ($HOCH_2CH_2SH$) monolayer adsorbed on a gold electrode in 0.5 mol l^{-1} KOH solution and observed two bands at 1549 and 1386 cm^{-1} which they attributed to the asymmetric and symmetric, respectively, stretches of carboxylate species.[95] Although the band at lower frequency was found near to the band at 1383 cm^{-1} observed in the present study, the band at higher frequency was not observed in the present study. Thus, the decomposed product of the present study was not carboxylate. Possible reasons for the different oxidation products include the different oxidation mechanism for the alkanethiol monolayer with different lengths of alkyl chains and the difference in the terminal group. Details of the effect of the terminal group on the oxidative decomposition mechanism are now under investigation. It should be stressed here that this is the first IR spectroscopic evidence for the formation of alkylsulfonic acid as one of the oxidative desorption products of the self-assembled monolayer of alkylthiolate.

The band at 2342 cm^{-1} was observed clearly by both p- and s-polarization as soon as the oxidation of the monolayer commenced (Fig. 8 and 9) and may be attributed to the IR absorption by CO_2 in the solution. This band was also observed during the anodic oxidative desorption of the nitrile and ferrocene terminated alkyl thiolate monolayers on the gold electrode.[56,75] CO_2 is the product of complete oxidative decomposition of the thiol monolayer.

Walczak *et al.* reported that the alkanthiolate monolayer is desorbed directly from the electrode at cathodic potential region in alkaline solution (pH > 11)[82] but the above results show that the oxidative anodic decomposition process in acidic media is much more complicated. The observation of stretching band of R—SO_3H as well as C—H in s-polarized spectra clearly show the existence of R—SO_3H species in solution. This suggests that the initial stage of the oxidative decomposition process is the anodic cleavage of S—Au to form R—SO_3H. This species stays near the electrode possibly within the monolayer and is further oxidized to CO_2. The detailed mechanism for the CO_2 generation from the monolayer with long alkyl chain is not very clear at this stage and further study is now in progress.

Conclusion

In summary, a new hydroquinone-terminated self-assembled monolayer, 2-(11-mercaptoundecyl)hydroquinone ($H_2QC_{11}SH$), was constructed on a gold electrode surface. The structural change of the monolayer during the redox reaction of the terminal quinone group and the irreversible oxidative decomposition process in 0.1 mol l^{-1} $HClO_4$ solution were investigated by electrochemical *in situ* FT-IRRAS measurement. It was found that IR bands observed by p-polarized measurement in the frequency region of 1700–1100 cm^{-1} corresponded well to the redox reaction of the terminal quinone moiety in the monolayer. From the time-dependent FT-IRRAS measurement, it was found that both the oxidation and reduction reactions were slow and reduction of quinone in the monolayer was slower than the oxidation of the hydroquinone group. When a potential more positive than +1.4 V was applied, the monolayer was oxidized irreversibly, the IR

bands in the frequency region of 1700–1100 cm^{-1} in the p-polarization spectra started to decrease and the bands at the same position appeared in the s-polarization spectra. A number of new bands due to the C—H stretch, SO_2 stretch of alkylsulfonic acid and CO_2 were also observed in this anodic potential region. These results suggest that the $H_2QC_{11}SH$ monolayer was oxidized by anodic cleavage of the S—Au bond to form alkylsulfonic acid which possibly existed within the partially decomposed monolayer and was further oxidized to CO_2.

This work was partially supported by Grant-in-Aid for Scientific Research (07750904), for Priority Area Research (05235201, 06226201, 07215202, 07241203, 08231203) and the International Scientific Research Program (Joint Research 07044046) from the Ministry of Education, Science, Sports and Culture, Japan.

References

1 F. Haber and R. Russ, *Z. Phys. Chem.*, 1904, **47**, 2527.
2 K. J. Vetter, *Z. Elektrochem.*, 1952, **56**, 797.
3 K. J. Vetter, *Electrochemical Kinetics*, Academic Press, New York, 1967.
4 B. R. Eggins and J. Q. Chamber, *J. Electrochem. Soc.*, 1970, **117**, 186.
5 J. H. Hale and R. Persons, *Trans. Faraday Soc.*, 1963, **59**, 1429.
6 J. Q. Chambers, *Electrochemistry of Quinones in the Chemistry of the Quinonoid Compounds*, ed. S. Patai, Wiley, New York, 1974.
7 E. Laviron, *J. Electroanal. Chem.*, 1983, **146**, 15.
8 E. Laviron, *J. Electroanal. Chem.*, 1984, **164**, 213.
9 M. Davies and F. E. Prichard, *Trans. Faraday Soc.*, 1963, **59**, 1248.
10 B. R. Clark and D. H. Evans, *J. Electroanal. Chem.*, 1976, **69**, 181.
11 R. S. K. A. Gamage, S. Umapathy and A. J. McQuillan, *J. Electroanal. Chem.*, 1990, **284**, 229.
12 M. Bauscher and W. Mäntele, *J. Phys. Chem.* 1992, **96**, 11101.
13 E. B. Troughton, C. B. Bain, G. M. Whitesides, R. G. Nuzzo, D. L. Allara and M. D. Porter, *Langmuir*, 1988, **4**, 365.
14 G. M. Whitesides and P. E. Laibinis, *Langmuir*, 1990, **6**, 87, and references therein.
15 A. Ulman, *An Introduction to Ultra-thin Organic Films From Langmuir–Blodgett to Self-assembly*, Academic Press, San Diego, 1991.
16 T. T. Li and M. J. Weaver, *J. Am. Chem. Soc.*, 1984, **106**, 1233; **106**, 6107.
17 H. O. Finklea, S. Avery, M. Lynch and T. Furtsch, *Langmuir*, 1987, **3**, 409.
18 H. C. D. Long, J. J. Donohue and D. A. Buttry, *Langmuir*, 1991, **7**, 2196.
19 K. Uosaki, Y. Sato and H. Kita, *Langmuir*, 1991, **7**, 1510.
20 K. Uosaki, Y. Sato and H. Kita, *Electrochim. Acta*, 1991, **36**, 1799.
21 H. O. Finklea and D. D. Hanshew, *J. Am. Chem. Soc.*, 1992, **114**, 3173.
22 K. Shimazu, Y. Yagi, Y. Sato and K. Uosaki, *Langmuir*, 1992, **8**, 1385.
23 J. A. M. Sondag-Huethorst and L. G. J. Fokkink, *Langmuir*, 1994, **10**, 4380.
24 D. L. Allara and R. G. Nuzzo, *Langmuir*, 1985, **1**, 52.
25 R. G. Nuzzo, F. A. Fusco and D. L. Allara, *J. Am. Chem. Soc.*, 1987, **109**, 2358.
26 M. D. Porter, T. B. Bright, D. L. Allara and C. E. D. Chidsey, *J. Am. Chem. Soc.*, 1987, **109**, 3559.
27 C. E. D. Chidsey and D. N. Loiacono, *Langmuir*, 1990, **6**, 682.
28 B. J. Barner and R. M. Corn, *Langmuir*, 1990, **6**, 1023.
29 R. G. Nuzzo, L. H. Dubois and D. L. Allara, *J. Am. Chem. Soc.*, 1990, **112**, 558.
30 M. M. Walczak, C. Chung, S. M. Stole, C. A. Widrig and M. D. Porter, *J. Am. Chem. Soc.*, 1991, **113**, 2370.
31 B. J. Barner, M. J. Green, E. I. Saez and R. M. Corn, *Anal. Chem.*, 1991, **63**, 55.
32 S. E. Creager and C. M. Steiger, *Langmuir*, 1995, **11**, 1852.
33 K. Sinniah, J. Cheng, S. Terrettaz, J. E. Reutt-Robey and C. J. Miller, *J. Phys. Chem.*, 1995, **99**, 14500.
34 P. E. Laibinis, C. D. Bain, R. G. Nuzzo and G. M. Whitesides, *J. Phys. Chem.*, 1995, **99**, 7663.
35 S. M. Stole and M. D. Porter, *Langmuir*, 1990, **6**, 1199.
36 D. D. Popenone, R. S. Deinhammer and M. D. Porter, *Langmuir*, 1992, **8**, 2521.
37 M. R. Anderson and M. Gatin, *Langmuir*, 1994, **10**, 1638.
38 J. A. Mielczarski, E. Mielzarski, J. Zachwieja and J. M. Gases, *Langmuir*, 1995, **11**, 2787.
39 T. Ohtsuka, Y. Sato and K. Uosaki, *Langmuir*, 1994, **10**, 3658.
40 K. Shimazu, S. Ye, Y. Sato and K. Uosaki, *J. Electroanal. Chem.*, 1994, **375**, 409.
41 D. A. Stern, E. Wellner, G. N. Salaita, L. L. Davidson, F. Lu, D. G. Frank, D. C. Zapien, N. Walton and A. T. Hubbard, *J. Am. Chem. Soc.*, 1988, **110**, 4885.
42 A. T. Hubbard, *Chem. Rev.*, 1988, **88**, 633.
43 M. P. Soriaga, J. L. Stickney and A. T. Hubbard, *J. Electroanal. Chem.*, 1983, **144**, 207.
44 M. P. Soriaga, P. H. Wilson and A. T. Hubbard, *J. Electroanal. Chem.*, 1982, **142**, 317.
45 M. P. Soriaga and A. T. Hubbard, *J. Am. Chem. Soc.*, 1982, **104**, 3937.
46 A. T. Hubbard, J. L. Stickney, M. P. Soriaga, V. K. F. Chia, S. D. Rosasco, B. C. Schardt, T. Solomun, D. Song, J. H. White and A. Wieckowski, *J. Electroanal. Chem.*, 1984, **168**, 43.
47 B. G. Bravo, T. Mebrahtu, M. P. Soriaga, D. C. Zapien, A. T. Hubbard and J. L. Stickney, *Langmuir*, 1987, **3**, 595.
48 T. Mebrahtu, G. M. Buttry, B. G. Bravo, S. L. Michelnaugh and M. P. Soriaga, *Langmuir*, 1988, **4**, 1147.
49 Y. Sato, M. Fujita, F. Mizutani and K. Uosaki, *J. Electroanal. Chem.*, 1996, **409**, 145.
50 J. J. Hickman, D. Offer, P. E. Laibinis, G. M. Whitesides and M. S. Wrighton, *Science*, 1991, **252**, 688.
51 K. Uosaki, A. Yasiro and Y. Sato, in preparation.
52 L. Zhang, T. Lu, G. W. Gokel and A. F. Kafer, *Langmuir*, 1993, **9**, 786.
53 Y. Mo, M. Sabdifer, C. Sukenik, R. J. Barriga, M. P. Soriaga and D. A. Scherson, *Langmuir*, 1995, **11**, 4626.
54 T. Sasaki, I. T. Bae, D. A. Scherson, B. G. Bravo and M. P. Soriaga, *Langmuir*, 1990, **6**, 1234.
55 I. T. Bae, M. Sandifer, Y. W. Lee, D. A. Tryk, C. N. Sukenik and D. A. Scherson, *Anal. Chem.*, 1995, **67**, 4508.
56 Y. Sato, S. Ye, T. Haba and K. Uosaki, *Langmuir*, 1996, **12**, 2726.
57 B. Beden and C. Lamy, in *Spectroelectrochemistry*, ed. R. J. Gale, Plenum Press, New York, 1988, ch. 5.
58 K. Ashley, F. M. Weinert, M. G. Samant, H. Seki and M. R. Philpott, *J. Phys. Chem.*, 1991, **95**, 7409.
59 K. Kunimatsu, M. G. Samant, H. Seki and M. R. Philpott, *J. Electroanal. Chem.*, 1988, **258**, 163.
60 P. W. Faguy, N. Markovic, P. R. Adzic, C. A. Fierro and F. B. Yeager, *J. Electroanal. Chem.*, 1990, **289**, 245.
61 T. Iwasita and F. C. Nart, *J. Electroanal. Chem.*, 1990, **295**, 215.
62 V. B. Paulissen and C. Koreniewski, *J. Electroanal. Chem.*, 1990, **290**, 18.
63 S. Ye, H. Kita and A. Aramata, *J. Electroanal. Chem.*, 1992, **333**, 299.
64 F. C. Nart, T. Iwasita and M. Weber, *Ber. Bunsen-Ges. Phys. Chem.*, 1993, **97**, 737.
65 B. Beden, C. Lamy, C. Bewick and K. Kunimatsu, *J. Electroanal. Chem.*, 1981, **121**, 343.
66 K. Kunimatsu, W. G. Golden and H. Seki, *Langmuir*, 1985, **1**, 245.
67 K. Kunimatsu, *J. Phys. Chem.*, 1984, **88**, 2195.
68 J. Clavilier, R. Faure, G. Guinet and R. Durand, *J. Electroanal. Chem.*, 1980, **107**, 205.
69 N. B. Colthup, L. H. Daly and S. E. Wiberley, *Introduction to Infrared and Raman Spectroscopy*, Academic Press, New York, 1st edn., 1964.
70 R. M. Silverstein, G. C. Bassler and T. C. Morrill, *Spectrometric Identification of Organic Compounds*, 4th edn., Wiley, 1991.
71 C. J. Pouchert, *The Aldrich Library of Infrared Spectra*, Aldrich Co., Milwaukee, 3rd edn., 1981.
72 E. Laviron, *J. Electroanal. Chem.*, 1979, **101**, 19.
73 H. Angerstein-Kozlowska, J. Klinger and B. E. Conway, *J. Electroanal. Chem.*, 1977, **75**, 45.
74 S. Srinivasan and E. Giliedi, *Electrochim. Acta*, 1966, **11**, 321.
75 S. Ye, T. Haba and K. Uosaki, in preparation.
76 K. Nakamoto, *Infrared and Raman Spectra of Inorganic and Coordination Compounds*, Wiley, 1986.
77 R. C. Weast, *CRC Handbook of Chemistry and Physics*, CRC Press, Cleveland, 1980.
78 R. N. Adams, *Electrochemistry on Solid Electrode*, Marcel Dekker, New York, 1969.
79 W. Flaaig, H. Beutelspacher, H. Riemer and E. Kalke, *Liebig's Ann. Chem.*, 1968, **719**, 96.

80 R. G. Greenler, *J. Chem. Phys.*, 1966, **44**, 310.
81 C. A. Widrig, C. Chung and M. D. Porter, *J. Electroanal. Chem.*, 1991, **310**, 335.
82 M. M. Walczak, D. D. Popenoe, R. S. Denhammer, B. D. Lamp, C. Chung and M. D. Porter, *Langmuir*, 1991, **7**, 2687.
83 J. Huang, J. C. Hemminger, *J. Am. Chem. Soc.*, 1993, **115**, 5305.
84 Y. Li, J. Huang, R. T. McIver, Jr. and J. C. Hemminger, *J. Am. Chem. Soc.*, 1992, **114**, 2428.
85 J. Huang, D. A. Dahlgren and J. C. Hemminger, *Langmuir*, 1994, **10**, 626.
86 D. Barnard, J. M. Fabian and H. P. Koch, *J. Chem. Soc.*, 1949, 2442.
87 S. Detoni and D. Hadzi, *Spectrochim. Acta*, 1957, **11**, 601.
88 L. J. Bellamy and R. L. Williams, *J. Chem. Soc.*, 1957, 863.
89 L. W. Daasch, *Spectrochim. Acta*, 1958, **13**, 257.
90 E. Merian, *Helv. Chim. Acta*, 1960, **43**, 1122.
91 N. S. Ham, A. N. Hambly and R. H. Laby, *Aust. J. Chem.*, 1960, **13**, 443.
92 G. Geiseler and K. O. Bindernagel, *Z. Elektrochem.*, 1960, **64**, 421.
93 E. A. Robinson, *Can. J. Chem.*, 1961, **39**, 247.
94 B. J. Lindberg, *Acta Chem. Scand.*, 1967, **21**, 2215.
95 D. E. Weisshaar, M. M. Walczak and M. D. Porter, *Langmuir*, 1993, **9**, 323.

Paper 6/02329K; *Received* 3*rd April*, 1996